Deep-Sea Research I 58 (2011) 524–534

Contents lists available at ScienceDirect

Deep-Sea Research I

journal homepage: www.elsevier.com/locate/dsri

Formation rates of Subantarctic mode water and Antarctic intermediate water within the South Pacific

Corinne A. Hartin [a,*], Rana A. Fine [a], Bernadette M. Sloyan [b,c], Lynne D. Talley [d], Teresa K. Chereskin [d], James Happell [a]

[a] Rosenstiel School of Marine and Atmospheric Science, University of Miami, 4600 Rickenbacker Causeway, Miami, FL 33149-1098, USA
[b] Centre for Australian Weather and Climate Research, CSIRO Marine and Atmospheric Research, Hobart, Tasmania, Australia
[c] CSIRO Wealth from Oceans National Research Flagship, Hobart, Tasmania, Australia
[d] Scripps Institution of Oceanography, University of California San Diego, 9500 Gilman Drive, La Jolla, CA 92093-0230, USA

ARTICLE INFO

Article history:
Received 27 September 2010
Received in revised form
21 February 2011
Accepted 24 February 2011
Available online 8 March 2011

Keywords:
CFCs
Antarctic intermediate water
Subantarctic mode water
South Pacific Ocean
Formation rate

ABSTRACT

The formation of Subantarctic Mode Water (SAMW) and Antarctic Intermediate Water (AAIW) significantly contributes to the total uptake and storage of anthropogenic gases, such as CO_2 and chlorofluorocarbons (CFCs), within the world's oceans. SAMW and AAIW formation rates in the South Pacific are quantified based on CFC-12 inventories using hydrographic data from WOCE, CLIVAR, and data collected in the austral winter of 2005. This study documents the first wintertime observations of CFC-11 and CFC-12 saturations with respect to the 2005 atmosphere in the formation region of the southeast Pacific for SAMW and AAIW. SAMW is 94% and 95% saturated for CFC-11 and CFC-12, respectively, and AAIW is 60% saturated for both CFC-11 and CFC-12. SAMW is defined from the Subantarctic Front to the equator between potential densities 26.80–27.06 kg m^{-3}, and AAIW is defined from the Polar Front to 20°N between potential densities 27.06–27.40 kg m^{-3}. CFC-12 inventories are 16.0×10^6 moles for SAMW and 8.7×10^6 moles for AAIW, corresponding to formation rates of 7.3 ± 2.1 Sv for SAMW and 5.8 ± 1.7 Sv for AAIW circulating within the South Pacific. Inter-ocean transports of SAMW from the South Pacific to the South Atlantic are estimated to be 4.4 ± 0.6 Sv. Thus, the total formation of SAMW in the South Pacific is approximately 11.7 ± 2.2 Sv. These formation rates represent the average formation rates over the major period of CFC input, from 1970 to 2005. The CFC-12 inventory maps provide direct evidence for two areas of formation of SAMW, one in the southeast Pacific and one in the central Pacific. Furthermore, eddies in the central Pacific containing high CFC concentrations may contribute to SAMW and to a lesser extent AAIW formation. These CFC-derived rates provide a baseline with which to compare past and future formation rates of SAMW and AAIW.

1. Introduction

Subantarctic Mode Water (SAMW) and Antarctic Intermediate Water (AAIW) are large-volume relatively cool water masses, which in their formation regions sequester significant quantities of atmospheric gases, e.g. CO_2 and chlorofluorocarbons (CFCs) (Fine et al., 2001; Sabine et al., 2004; Willey et al., 2004). Past changes in global atmospheric CO_2 concentrations over interglacial and glacial cycles may have been driven by changes in ventilation and circulation of intermediate and deep waters (e.g., Siegenthaler and Wenk, 1984; Francois et al., 1997; Toggweiler, 1999). In the present ocean, the formation and circulation of SAMW and AAIW are an important component of the upper branch of the meridional overturning circulation (MOC), involved in the transport of heat and salt within the southern hemisphere subtropical gyre (Schmitz, 1996; Sloyan and Rintoul, 2001a; Talley, 2003, 2008).

There are numerous processes that influence the formation and properties of SAMW and AAIW, convection within mixed layers due to air-sea fluxes, Ekman transport, eddy fluxes, and mixing within the Subantarctic Front (SAF; McCartney, 1982; Sloyan and Rintoul, 2001b; Sloyan et al., 2010; Sallee et al., 2010a). Circumpolar Deep Water upwells around Antarctica and is carried northward via Ekman transport as Antarctic Surface Water (AASW). AASW is converted to AAIW through air-sea fluxes equatorward of the Polar Front (PF) and subducts at the Subantarctic Front (SAF; e.g., Sloyan and Rintoul, 2001b). AAIW is characterized by a vertical salinity minimum and observed in the southern hemisphere oceans between 600 and 1100 m (e.g. Hanawa and Talley, 2001). Equatorward of AAIW formation, SAMW is formed from the deepening of mixed layers during wintertime convection (Holte et al., submitted for publication) and subsequent mixing (Sloyan et al., 2010), and is found north of the SAF throughout the southern hemisphere. SAMW is characterized by

* Corresponding author. Tel.: +1 305 421 4718; fax: +1 305 421 4689.
E-mail address: chartin@rsmas.miami.edu (C.A. Hartin).

0967-0637/$ - see front matter © 2011 Elsevier Ltd. All rights reserved.
doi:10.1016/j.dsr.2011.02.010

a minimum in potential vorticity. It occupies the lower pycnocline of the southern hemisphere subtropical gyres. As a consequence of the formation process, both SAMW and AAIW have relatively high gas concentrations—oxygen, CO_2 and CFCs. SAMW and AAIW are transported eastward with the Antarctic Circumpolar Current (ACC) and northward into the Indian, Pacific, and Atlantic subtropical gyres. The coldest and freshest variety of SAMW is formed in the southeast Pacific (McCartney, 1977, 1982), the main region supplying SAMW and AAIW to the Pacific.

Chlorofluorocarbons (CFC-11 and CFC-12) are oceanic tracers used to evaluate circulation patterns, ages, and formation rates of water masses (e.g., Fine, 2011). CFCs are anthropogenic compounds that have been continuously added to the atmosphere since the 1930s. The concentrations have been increasing in the atmosphere up to the late 1990s for CFC-11 and to the early 2000s for CFC-12. The largest increase in concentration has occurred since the 1970s. The CFCs enter the surface ocean from the atmosphere by gas exchange, with an average equilibration time of about 1 month (Broecker et al., 1980). Once they become isolated from the atmosphere, CFC concentrations are stable in the ocean interior, except for the effects of mixing with waters of different concentrations. Most surface waters are found to be close to saturation with respect to the atmosphere. However, this varies in regions of deep convection and vertical mixing, where mixed layers maybe too deep to maintain equilibrium with the atmosphere (Smethie and Fine, 2001). It is the surface saturations together with total inventories of CFCs that are critical in calculating the ages and formation rates of water masses.

In this study, we use the first austral wintertime observations of CFC-11 and CFC-12 concentrations in the southeast Pacific for SAMW and AAIW to determine the percent saturation of CFC-11 and CFC-12 relative to the present atmosphere. Formation rates are calculated for SAMW and AAIW from 1970 to 2005. Formation rates are directly related to the percent saturation during winter water mass formation and to the total inventory of CFCs within each water mass. Inter-oceanic transports of SAMW and AAIW are calculated to estimate the potential loss of SAMW and AAIW out of the South Pacific through the Drake Passage. This paper will also address the location of formation areas of SAMW and AAIW, and the possible impact of eddies on formation of SAMW and AAIW within the South Pacific. Finally, SAMW and AAIW in the South Pacific will be compared with mode and intermediate waters globally.

2. SAMW and AAIW in the South Pacific

2.1. Hydrographic and chlorofluorocarbon data

World Ocean Circulation Experiment (WOCE) and Climate Variability and Prediction (CLIVAR) tracer and hydrographic data, and data collected on board the *R/V Knorr* between August and October of 2005 in the southeast Pacific (SAMFLOC; Chereskin, 2005) are used in this analysis (Fig. 1). [Data are available at http://cchdp.ucsd.edu/]. The WOCE and CLIVAR observations date from 1989 to 2006, and are located between 70°S and 20°N and 70°W and 150°E. A total of 4732 individual CFC-12 measurements at 327 stations are used in the inventory calculation for SAMW, and 5558 individual CFC-12 measurements at 355 stations for AAIW. Challenges associated with combining data from multiple years are discussed in Section 3.1.

2.2. Water mass boundaries

To calculate the CFC-12 inventories within SAMW and AAIW, water mass boundaries are determined from examining the WOCE, CLIVAR, and the 2005 SAMFLOC data. Boundaries are chosen based on a combination of numerous parameters including: temperature, salinity, potential vorticity, nutrients, oxygen, CFC-11 and CFC-12

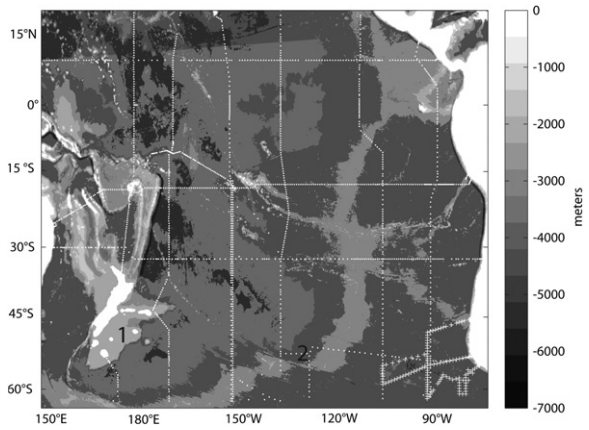

Fig. 1. Map of the South Pacific with grayscale shading representing bottom bathymetry (m) from ETOPO2. Diamonds represent the location of the hydrographic profiles from WOCE and CLIVAR with 150°W occupied during 1991 and 2005, and the crosses represent the station locations from the 2005 SAMFLOC cruise. The number 1 identifies the location of the Campbell Plateau and number 2 identifies the Eltanin Fracture Zone.

concentrations and saturations (Table 1). SAMW lies between potential densities (σ_θ) $26.80 < \sigma_\theta \leq 27.06$ kg m^{-3} and is characterized by a minimum in potential vorticity, outcropping north of the SAF and forming within mixed layers exceeding 400 m during the austral winter (Fig. 2a). SAMW subducts to a depth of ~600 m, and is integrated into the subtropical gyre of the South Pacific. The isopycnal 26.80 kg m^{-3} separates SAMW from the lighter thermocline waters of the South Pacific. The isopycnal 27.06 kg m^{-3} is the base of the potential vorticity minimum and also separates SAMW from the denser AAIW found between $27.06 < \sigma_\theta \leq 27.20$ kg m^{-3}. Other observational studies have defined SAMW and AAIW on similar density surfaces. For example, Tsuchiya and Talley (1998) define SAMW between 26.9 and 27.1 kg m^{-3} and AAIW between 27.0 and 27.35 kg m^{-3} along 88°W in the South Pacific. AAIW is characterized by a salinity minimum, outcropping at the Polar Front (PF) during austral winter and subducting to depths of 1100–1200 m. Fig. 2b shows the low salinity signal of AAIW within the upper few hundred meters subducting at the SAF. As AAIW is transported equatorward within the subtropical gyre, the density increases and the salinity minimum broadens in density from 27.06–27.40 kg m^{-3} (e.g. Reid, 1965).

2.3. CFC and oxygen saturations in the southeast Pacific in austral winter 2005

This is the first study to document CFC-11 and CFC-12 saturations in SAMW and AAIW in austral winter in the southeast Pacific. Saturations are calculated (Warner and Weiss, 1985) from the 2005 winter data by comparing the measured oceanic concentrations to the atmospheric concentrations from the ALE/GAGE/AGAGE network (http://cdiac.ornl.gov/ndps/alegage.html), a global network of trace atmospheric gas measurements. In this paper, surface waters represent the upper 10 m of the water column.

From the austral winter 2005 SAMFLOC data, we observe average CFC-11, CFC-12, and O_2 surface saturations (not shown) poleward of the SAF to be slightly undersaturated. Within the mixed layers of SAMW (26.80 and 27.06 kg m^{-3}), CFC-11 and CFC-12 are 94% and 95% saturated with respect to the 2005 atmosphere (Fig. 3a), respectively. Within the core of AAIW (27.20 kg m^{-3}) poleward of the SAF, AAIW is 85% saturated in CFC-12 relative to the present atmosphere (Fig. 3b), and average oxygen saturations are 79%. Once AAIW subducts under the SAF, average CFC-11 and CFC-12 saturations decrease dramatically to

Table 1
Average properties of SAMW and AAIW from the SAMFLOC 2005 austral winter data in the southeast Pacific from approximately 76°W to 100°W and from 60°S to 45°S. Average properties are taken when the density range for SAMW is within the mixed layer, and average properties for AAIW are taken within the density range for AAIW, north of the SAF.

	Density ($kg\ m^{-3}$)	Potential temperature (°C)	Salinity (psu)	PV ($10^{-12}\ m^{-1}\ s^{-1}$)	CFC-11 ($pmol\ kg^{-1}$)	CFC-12 ($pmol\ kg^{-1}$)	O_2 ($\mu mol\ kg^{-1}$)	CFC-11% saturation	CFC-12% saturation	O_2% saturation
SAMW	26.8–27.06	5.2	34.15	<10	4.6	2.5	300	94	95	97
AAIW	27.06–27.40	4.0	34.20	~ 70	3.0	1.5	250	60	60	79

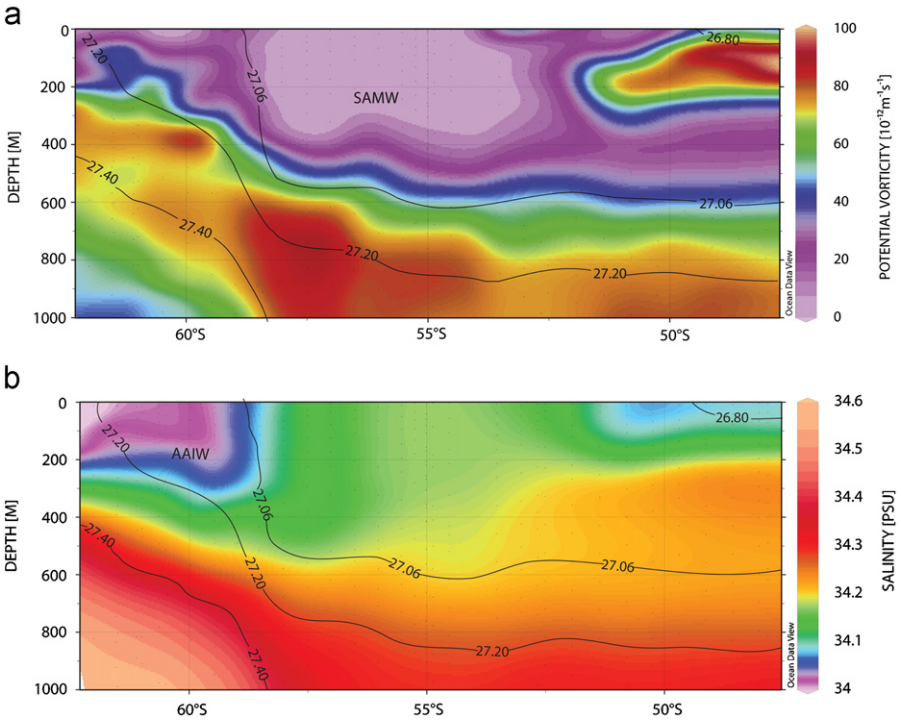

Fig. 2. Depth sections along 88°W from August 2005 of (a) potential vorticity and (b) salinity. SAMW lies between 26.8–27.06 $kg\ m^{-3}$, AAIW lies between 27.06–27.2 $kg\ m^{-3}$ and extends down to 27.4 $kg\ m^{-3}$ within the subtropical gyre. The location of the SAF is found at the outcrop of 27.06 $kg\ m^{-3}$, approximately 59°S.

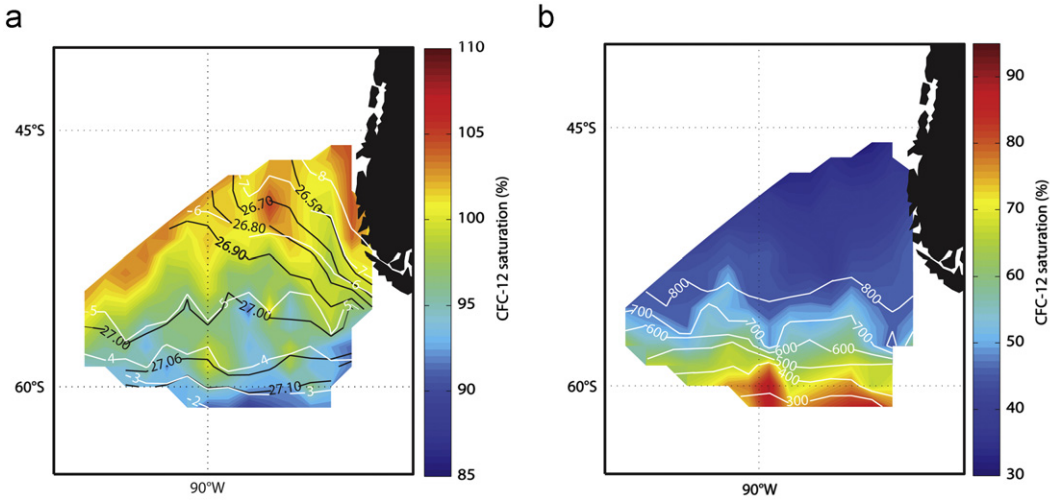

Fig. 3. (a) Colored contour represents CFC-12 surface saturations (%) relative to the 2005 atmosphere from the 2005 data. Black contours represent density in $kg\ m^{-3}$, and white contours are potential temperature in °C. The approximate location of the SAF during the 2005 cruise is along the 4 °C isotherm. (b) Colored contours represent CFC-12 saturations along 27.2 $kg\ m^{-3}$ (the core of AAIW). White contours are the depth of the 27.2 $kg\ m^{-3}$ isopycnal. The approximate location of the SAF during the 2005 cruise is along the 600 m contour. Note the change in CFC-12 saturations poleward and equatorward of the SAF. There is a scale change between (a) and (b).

less than 60%, due to mixing near the front (Sloyan et al., 2010). The 60% saturation for AAIW in late winter north of the SAF is similar to that observed for recently formed Labrador Sea Water in 1500 m mixed layers, though formation mechanisms are somewhat different (Wallace and Lazier, 1988; Rhein et al., 2002).

3. CFC-12 inventories

CFC-12 inventories are calculated for SAMW and AAIW using a technique described in earlier work (Orsi et al., 1999; Smethie and Fine, 2001; Rhein et al., 2002; LeBel et al., 2008):

$$CFC_{inv} = \rho \Sigma([CFC]_{(ij)} AD_{(ij)}) \quad (1)$$

where CFC_{inv} is the CFC-12 inventory in moles, ρ is the density of water (kg m^{-3}), $[CFC]_{(ij)}$ is the CFC-12 concentration (pmol kg^{-1}) at latitude (i) and longitude (j), A (m^2) is the area of the grid box ($2.5^\circ \times 5^\circ$, from Willey et al., 2004), and $D_{(ij)}$ (m) is the thickness of each layer at a location i and j. The inventories for SAMW (26.80–27.06 kg m^{-3}) are calculated between the SAF and the equator, and for AAIW (27.06–27.40 kg m^{-3}), from the PF to 20°N. The boundaries for both SAMW and AAIW extend from 150°E to 70°W. Temperature, salinity, and density data along each meridional WOCE and CLIVAR section are analyzed to determine if the location of the SAF and PF are significantly different than the climatological mean location from Orsi et al. (1995). The only significant difference was along 170°W, where the location of the PF was approximately 5° north of the Orsi et al. (1995) mean. Stations located south of the SAF for SAMW and south of the PF for AAIW are not included in the inventory calculations.

The total CFC-12 normalized inventory (see Section 3.1 for normalization technique) for SAMW between 26.80 and 27.06 kg m^{-3} is 16.0×10^6 moles. The total inventory for AAIW between 27.06 and 27.40 kg m^{-3} is 8.7×10^6 moles. The inventory map (Fig. 4a) is smoothed based on a two dimensional running mean of the gridded CFC-12 inventories within SAMW. The technique reduces the CFC-12 inventory maxima. Therefore, the maximum CFC-12 inventory at a hydrographic station are 4.6 mol km^{-2} within the original data, 2.0 mol km^{-2} within the gridded data, and 0.77 mol km^{-2} within the two dimensional smoothed data. The smoothed data are used as they provide a more continuous picture of the CFC-12 inventory extrema over the South Pacific. As with SAMW, the AAIW inventory map (Fig. 4b) is smoothed both in latitude and

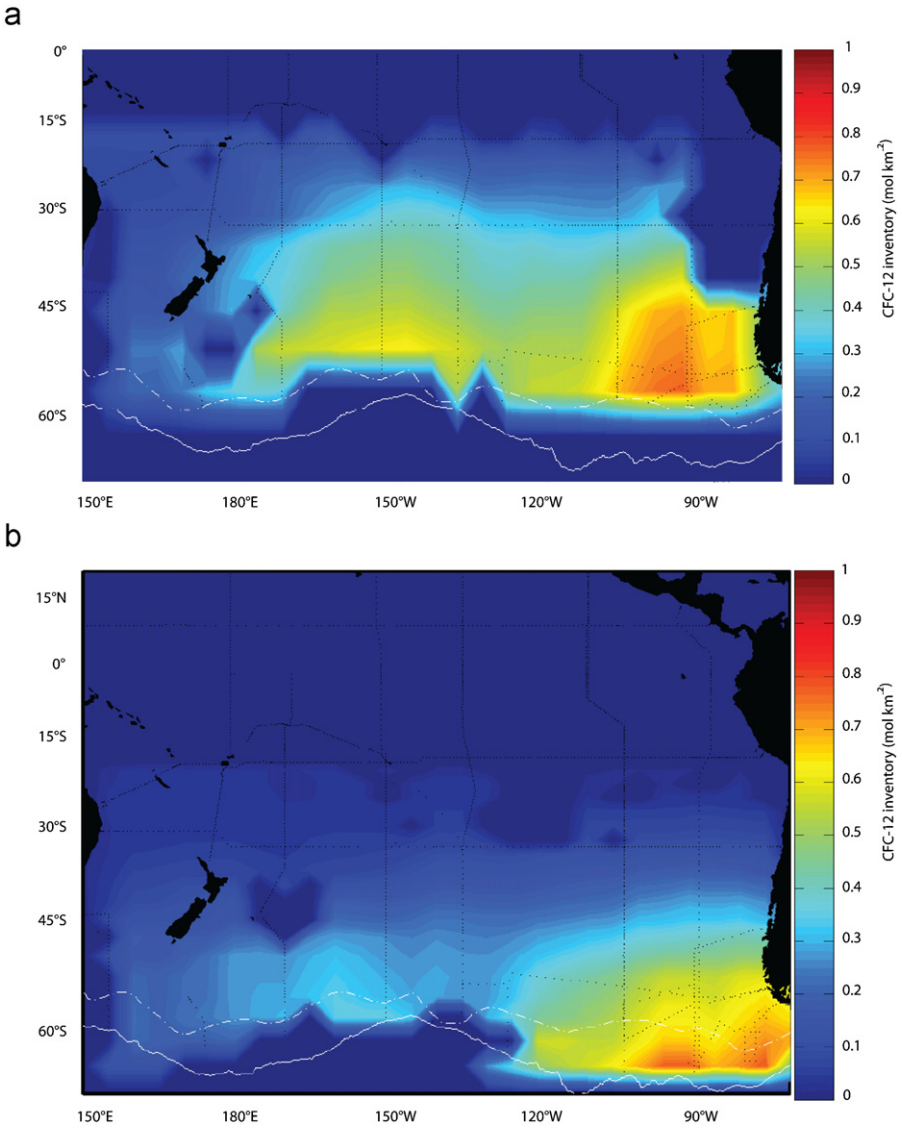

Fig. 4. CFC-12 inventory maps normalized to 2005 in mol km^{-2} for (a) SAMW from the SAF to the equator and, (b) AAIW, from the PF to 20°N. White dashed line is the mean location of the SAF and the white solid line is the mean location of the PF from Orsi et al. (1995).

longitude. The maximum CFC-12 inventory are 4.0 mol km^{-2} in the original data, 1.6 mol km^{-2} in the gridded data, and 0.79 mol km^{-2} in the gridded two dimensional smoothed data. The total CFC-12 inventories for SAMW and AAIW vary by $<1\%$ when using the smoothed or unsmoothed data.

3.1. Normalization of CFC inventories to the year 2005

The distribution of CFC data within the South Pacific spans 17 years, from 1989 to 2006. This presents a challenge in calculating a CFC inventory relative to a given date, as the atmospheric CFC concentrations vary with time (Walker et al., 2000). Therefore, the inventories at each station are normalized to a constant date in order to obtain a quasi-synoptic inventory of CFC-12. A constant date of January 1, 2005 is chosen because SAMFLOC data were collected in the austral winter of 2005. The technique used is similar to Smethie et al. (2000), where CFC-12 inventories at each station are scaled by a normalization factor.

In order to investigate the basin-wide circulation of SAMW and AAIW, pCFC-12 age maps along the core of each water mass are constructed (Fig. 5a and b). The age of the water masses are calculated at each hydrographic location within the South Pacific using the partial pressure (pCFC) method from Fine et al. (1988) and Doney and Bullister (1992);

$$pCFC = \frac{[CFC]}{F(\theta,S,sat)} \tag{2}$$

where [*CFC*] is the measured CFC-12 concentration in seawater, and *F* is the solubility from Warner and Weiss (1985) based on potential temperature (θ) and salinity (*S*), and *sat*, the saturation of CFC-12 at the formation region from the 2005 data. The equation does not take into account the path of the water parcel. The assumption is that the temperature and salinity do not change once leaving the formation region (see Section 5.1 for error analysis). The pCFC is compared to the atmospheric history to obtain a year of formation (Walker et al., 2000). This year of formation is then subtracted from present day to determine the age of the water mass. When the CFC-12 concentrations are <0.02 pmol kg^{-1}, ages are not calculated due to the large errors at these low concentrations (Smethie et al., 2000).

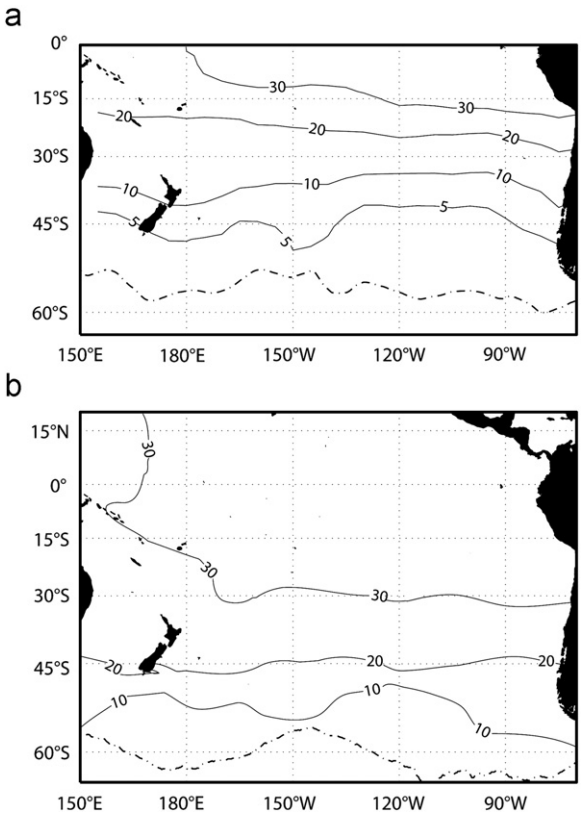

Fig. 5. CFC-12 relic age maps in years (a) for SAMW and (b) for AAIW. The dashed line in panel (a) is the location of the SAF and the dashed line in panel (b) is the location of the PF, from Orsi et al. (1995).

Typically the pCFC age at the region of formation is not zero due to mixing, dilution, and entrainment of older waters during formation. The non-zero formation age is known as the relic age of the water mass (e.g. Fine et al., 2002) and is subtracted from the pCFC age to properly account for water mass formation processes that cause undersaturation of CFC-12 in newly formed water masses. In this study, relic ages for SAMW and AAIW are 10 years and 15 years, respectively, estimated from the winter 2005 SAMFLOC data. The relic age of AAIW is greater than that of SAMW due to more significant mixing and entrainment of lower CFC-12 concentration waters as AAIW subducts below the SAF (Fig. 3b).

The relic corrected pCFC-12 ages are fairly zonal, with the youngest waters close to the source and progressively aging as distance from the source increases. This pattern allows for division of the South Pacific into seven meridional domains, in which the average annual percent change (p_c) for the year of formation is calculated over each domain. In other words, p_c is the amount the atmospheric CFC-12 changed in one year compared to the previous year:

$$p_c = \left(\frac{atm_2 - atm_1}{atm_1}\right) \times 100 \tag{3}$$

where atm_2 is the atmospheric concentration of the year of formation (Eq. (2)), and atm_1 is the atmospheric concentration of the previous year. The p_c is then used in the calculation of the normalization factors.

Normalization factors (N_f) are calculated using:

$$N_f = (Y_{2005} - Y_d)p_c \tag{4}$$

where Y_{2005} is the chosen constant date of 2005, Y_d is the date of the hydrographic cruise, and p_c is the annual atmospheric percent change for the year the water mass was formed (Eq. (3)) averaged over each domain. CFC-12 inventories at each station for SAMW and AAIW are normalized specifically to each cruise, rather than averaged. Data collected within one year of 2005 are not normalized. In principle, we modify the CFC data to become quasi-synoptic, as if they all were collected in 2005. As a check on the normalization process, inventories are also normalized to 1992. 1992 was the year with the most WOCE cruises over the South Pacific. Inventory patterns are similar using normalized data of 1992 (not shown) and 2005. Table 2 contains the average normalization factor within each domain, as well as the range of normalization factors.

4. Water mass formation rates

Average water mass formation rates over the period of CFC input, mostly since 1970, are calculated based on (Smethie and Fine, 2001; Kieke et al., 2006; LeBel et al., 2008)

$$R = \frac{CFC_{inv}}{\rho \int_{t_0}^{t_n} [C_s(t) sat] dt} \tag{5}$$

where CFC_{inv} is the normalized CFC-12 inventory from 2005 in moles, ρ is the density of water (kg m^{-3}), $C_s(t)$(pmol kg^{-1}) is the CFC-12 concentration at the source at 100% equilibrium with the atmosphere for the years 1970–2005, and *sat* is the percent CFC-12 saturation at

Table 2
Average normalization factors and range of normalization factors over the inventory domains for SAMW and AAIW. Each hydrographic station has its own factor based on time of cruise and relic age of water at that location.

Latitude	Longitude	SAMW average normalization factor	Range of normalization factors for SAMW	AAIW average normalization factor	Range of normalization factors for AAIW
64–54°S	75°W–150°E	1.06	1.05–1.07	1.14	1.11–1.15
54–45°S	75°W–150°E	1.15	1.12–1.16	1.25	1.19–1.26
45–36°S	75°W–150°E	1.45	1.36–1.54	1.60	1.48–1.73
36–27°S	75°W–150°E	1.77	1.55–1.84	1.90	1.66–1.99
27–18°S	75°W–150°E	2.01	1.78–2.19	2.05	1.81–2.23
18–0°S	75°W–150°E	2.31	2.04–2.60	2.17	1.07–2.43
0–20°N	75°W–150°E	–	–	–	–

the source, 95% and 60% for SAMW and AAIW, respectively. The assumptions are that the percent saturation at the time of formation and the formation rate are constant over the period of CFC input (see Section 5.3 for a discussion of errors associated with this assumption).

Based on this inventory, the water mass formation rate for SAMW remaining within the South Pacific is 7.3 ± 2.1 Sv ($1\ \text{Sv} = 10^6\ \text{m}^3\ \text{s}^{-1}$). The formation rate for AAIW is 5.8 ± 1.7 Sv (see Section 6 for error analysis). These rates represent the average formation rates for SAMW and AAIW within the South Pacific over the major period of CFC input from 1970 to 2005.

One potential influence on the formation rates not included is obduction. Obduction is the transfer of water from the permanent thermocline to the mixed layer above (Qiu and Huang, 1995). The process of obduction may affect the CFC saturation, influencing the inventories and formation rates. A flux of older water from the permanent thermocline into the mixed layer would result in CFC saturations significantly out of equilibrium with the present atmosphere. From the 2005 winter data, we find that within the mixed layers, CFC and oxygen saturations are close to equilibrium in the density range of SAMW and AAIW (Section 2.3). Thus, we assume that the effect of obduction on the CFC saturations is small.

There are regions of potential CFC loss from the layers of SAMW and AAIW and from the South Pacific. CFC concentrations are decreased within the layers of SAMW and AAIW by vertical mixing. While we cannot directly quantify this loss, observations show that CFC concentrations are at or close to zero below AAIW. Similarly, on SAMW and AAIW isopycnals in the Pacific subtropical gyre, CFC-12 concentrations are at or close to zero, northwest of 30°S, 160°E (not shown). These observations suggest that there is a minimal transfer of CFC-12 to the layers below and to the Indian Ocean via the Indonesian Throughflow. Furthermore, if concentrations of CFC-12 are near zero and are being mixed to layers below, these losses are insignificant to our inventory and formation rate calculations.

The total formation rate of SAMW and AAIW in the South Pacific additionally includes the portions that exit to the Atlantic Ocean through the Drake Passage (McCartney, 1977, 1982; Talley, 1996). To estimate the formation rates, we calculated volume transports along our winter 2005 77°W section from 55°S to 61°S, within the SAMW and AAIW layers. The meridian 77°W was chosen because it is the closest hydrographic section to the Drake Passage. Geostrophic transports were calculated relative to the bottom. We estimate that 4.4 ± 0.6 Sv of SAMW was transported across 77°W, comparable to the 4.8 ± 0.5 Sv reported by Sloyan and Rintoul (2001b) using an inverse model and an independent data set. Combining the formation rate of SAMW based on the CFC-12 inventory in the South Pacific subtropical gyre of 7.3 Sv with the geostrophic transport across 77°W of 4.4 Sv yields an average of 11.7 ± 2.2 Sv (see Section 5 for a full analysis of errors) of SAMW that is inferred to be forming in the southeast Pacific.

A total of 19.8 ± 2.0 Sv of AAIW was transported across 77°W in 2005, relative to the bottom. As AAIW is a small part of the large transport of the Subantarctic Zone, it is difficult to quantify how much newly formed AAIW is being transported through the Drake Passage. There is significant circumpolar-circulated AAIW within the ACC as well as recirculation of AAIW southward along the Chilean coast (Koshlyakov and Tarakanov, 2005). Thus, for AAIW we consider the 5.8 ± 1.7 Sv calculated from the South Pacific CFC inventory as a lower bound on the rate of AAIW formed in the southeast Pacific.

Error estimates on the transports are derived from Firing et al. (submitted for publication). They find a mean transport of 95 Sv with a standard deviation of 10 Sv from 51 direct velocity transects of the upper 1000 m of the Drake Passage, made over a period of 4.5 years. We estimate a total of 24.2 Sv ($4.4 + 19.8$ Sv) of SAMW and AAIW transported across 77°W. We scaled the standard deviation reported by Firing et al. (submitted for publication) by the transport ratio (24.2/95), assuming the error is distributed proportionately, to estimate an error of ± 2.5 Sv on the transports across 77°W. Our SAMW/AAIW transport estimate likely underestimates the transport because it is only the baroclinic component. However, since the error estimate is based on direct velocity observations, it included both barotropic and baroclinic variability. Also, the error may overestimate variability in the SAMW/AAIW transport, as the Firing et al. (submitted for publication) study included surface waters. There are a few studies that have looked at the total transport of SAMW and AAIW within the Drake Passage. Cunningham et al. (2003) find approximately 36 ± 2.7 Sv of SAMW and AAIW based on a series of sections within the Drake Passage from 1993 to 2000. Naveira Garabato et al. (2003) use an inverse model across multiple sections within the Drake Passage and find approximately 28 ± 2.5 Sv of SAMW and AAIW. Our transport is close to that found in Naveira Garabato et al. (2003). However, it is considerably less than the Cunningham et al. (2003) transport. Transports of SAMW and AAIW may increase once within the Drake Passage due to diapycnal diffusion, as was shown for AAIW in Naveira Garabato et al. (2003). We can see from these three studies that variability in the transport of SAMW and AAIW through the Drake Passage is small. This error estimate helps support our conclusion that 11.7 ± 2.2 Sv for SAMW is an average formation rate.

5. Error analysis

The error analysis follows that of LeBel et al. (2008). Significant errors in the formation rates result from three sources: errors related to CFC input, errors on the integrated inventories and their normalization to a constant date, and errors associated with assuming a constant formation rate over the period of the CFC input.

5.1. CFC input and solubility

The errors related to the CFC atmospheric source are due to the uncertainties in the atmospheric time history of the CFCs, and the

uncertainties related to the solubility of CFCs. Atmospheric time history errors are considered less than 1% after 1970 (Walker et al., 2000). The solubility of CFCs as a function of temperature and salinity is well known from laboratory measurements (Warner and Weiss, 1985). A change in temperature after leaving the formation region, which has the most effect on solubility, of 1–2 °C results in approximately 4–6% uncertainty in the solubility (Eq. (2)). Within the South Pacific, SAMW and AAIW change by approximately 1–2 °C between ~60°S and 20°S.

5.2. Integrated CFC inventories and time normalization

The sources of error in the CFC inventories are from measurement errors on individual seawater samples, errors due to normalizing data to a constant date, and errors due to limited spatial coverage. The measurement errors on individual samples are less than 2%, which propagate through the vertical integration to approximately 2% (Smethie and Fine, 2001). Errors from normalizing the data are estimated by comparing the CFC-12 concentrations of the normalized data to the original data from the occupations of P16, along 150°W, in 1991–1992, and in 2005–2006. The total average errors due to normalizing CFC-12 to a constant date are approximately 20% for both SAMW and AAIW.

Lastly, there are the errors associated with the spatial integration of the interpolated CFC-12 inventories. Regions of less dense sampling and of large CFC gradients will generate the most error in the CFC inventories (e.g. Waugh and Abraham, 2008). A bootstrap method is used in which 50% of the inventory data is randomly selected 100 times, gridded, and the root mean square variability (rms) is calculated for each grid point (Rhein et al., 2002; Kieke et al., 2006; LeBel et al., 2008). The resulting rms is a measure of the degree of uncertainty in the CFC-12 inventory due to the combined effects of the errors, non-synopticity of the cruises, large gradients in the data, and the spatial resolution of the data. The errors are 3% for SAMW and 6% for AAIW. Larger errors are associated with AAIW possibly due to stronger gradients in AAIW. These errors are the most conservative estimates, as they are based on the largest rms values.

5.3. Constant formation rate

In applying the CFC inventory method, percent saturation and formation rates are assumed to be constant over the time of CFC input, 1970s–2005. LeBel et al. (2008) and Smethie and Fine (2001) carried out elaborate sensitivity studies on Labrador Sea Water (LSW) to address this. While there is very well documented variability within LSW (Dickson et al., 1996; Lazier et al., 2002), there is only limited information on the variability of SAMW and AAIW.

Between 1993 and 2004, the South Pacific subtropical gyre wind-driven circulation increased by at least 20% (Roemmich et al., 2007). The increase in gyre circulation is attributed to an increase in the Southern Annular Mode (SAM) from 1990 to 1999, with a peak in 1998. During a positive SAM, subpolar westerlies increase with a resulting increase in the northward Ekman transport, as well as a global asymmetric deepening of the mixed layers affecting SAMW and AAIW (Hall and Visbeck, 2002; Naveira Garabato et al., 2009; Sallee et al., 2010b).

In this study, we use the Roemmich et al. (2007) circulation as an example of the potential effects of the SAM on intermediate water circulation and formation rates. We assume that a change in the wind forcing, along with a change in the mixed layer depth, will affect the formation of SAMW and AAIW, although we acknowledge that formation changes may not be uniform across the South Pacific (Sallee et al., 2010b). A sensitivity study is carried out to estimate the change in formation rates for SAMW and AAIW based on changes in the SAM. For lack of a better number, we used 20% from the Roemmich et al. (2007) circulation study and varied the formation rates over the SAM index (Marshall, 2003). We assume a linear response between SAM and the formation of SAMW and AAIW with no lag between the forcing and the response of SAMW and AAIW. The resulting formation rate for SAMW could then vary between 14.0 Sv (2003) to 9.4 Sv. For AAIW, the formation rate could vary between 7.0 Sv (2003) to 4.6 Sv.

5.4. Total error

The total error in the formation rates for SAMW and AAIW is calculated by combining the errors in CFC input and solubility, CFC inventories and normalization, and the assumption of constant formation rate. The errors are combined as the square root of the sum of the errors (Wolberg, 1967). These terms contribute a total error of 29% for SAMW and 30% for AAIW. The errors represent the most conservative estimates for the formation rates presented here.

6. Discussion

6.1. SAMW and AAIW formation areas

A map of the SAMW CFC-12 inventory (Fig. 4a) shows there are two areas of relative maxima (>0.6 mol km^{-2}), one centered on 90°W and the other centered on 150°W. We interpret these maxima as evidence of two main areas of SAMW formation in the Pacific sector of the Southern Ocean, consistent with the findings of McCartney (1982). Winter mixed layer depths greater than 400 m, equatorward of the SAF, are associated with each area (Holte et al., submitted for publication). In the Pacific the highest inventory of SAMW is centered on 90°W. This is visible from the inventory map with a large area of greater than 0.8 mol km^{-2} (Fig. 4a).

The second high CFC-12 inventory lies between about 170°W and 130°W, it is greater than 0.6 mol km^{-2}. This high inventory is consistent with the findings in Sallee et al. (2010a), of a new area of SAMW formation over the Eltanin Fracture Zone (140°W). However, Sallee et al. (2010a) do not find any formation of SAMW in the southeast Pacific, where this study finds the greatest Pacific inventory of CFC-12.

CFC-12 inventory maximum (>0.7 mol km^{-2}) for AAIW also lie within the southeast Pacific (100°W), poleward of SAMW (Fig. 4b). They are associated with low salinity at potential densities greater than 27.06 σ_θ, and are located south of the SAF. The maximum in the AAIW inventory in the southeast Pacific is consistent with previous findings (Iudicone et al., 2007), which report that the main site of AAIW formation is the southeast Pacific followed by AAIW transport into the subtropical gyres of both the Atlantic and Pacific.

For both SAMW and AAIW, more than 98% of the total CFC-12 inventory still remains poleward of 30°S. This high percentage is due to the significant uptake of gases near the fronts associated with the ACC and within the deep winter mixed layers. The substantial decrease equatorward of the maximum inventories is due to mixing with depleted CFC waters as SAMW and AAIW are transported northward from the fronts.

6.2. Mesoscale eddy influence on SAMW and AAIW formation

Within the original (non-gridded) inventories of SAMW and AAIW along 170°W and 150°W there are stations of higher than

average CFC-12 inventories. Upon close investigation of the hydrographic data and satellite images from the time of the 170°W cruise in 1996 and the 150°W cruise in 2005, these CFC-12 inventory maxima appear to be coincident with eddies. Hydrographic data, such as temperature, salinity, and density along the sections, suggest that these eddies are approximately two degrees in diameter. The properties within these eddies are similar to those found within SAMW and AAIW in the high CFC-12 inventories further to the east.

Between 170°W and 150°W, there were multiple cyclonic and anticyclonic eddies observed in 1996 and 2005. The cyclonic cold-core eddies are enriched in CFC concentrations (Fig. 6). Originating from the south, they apparently transport cold, gas enriched waters equatorward to influence properties of SAMW, as also observed south of Tasmania (Morrow et al., 2004; Herraiz-Borreguero and Rintoul, 2010). The anticyclonic eddies have the potential to be sites where CFCs are added through air-sea modification similar to what was observed south of Africa by Olson et al. (1992). In addition, in the Subantarctic Zone, the East Australian Current (EAC) is a source of warm and salty anticyclonic eddies influencing SAMW properties (Ridgway and Dunn, 2007). The Southern Ocean, and in particular the fronts associated with the ACC, are dominated by eddies, especially along 170°W, the Campbell Plateau, and the Australian sector of the Southern Ocean (e.g. Olson and Emery, 1978; Gille et al., 2000; Phillips and Rintoul, 2000). Eddies play a critical role in the stratification and circulation of the Southern Ocean, and have been shown to affect tracer and CO_2 distributions, as well as the formation of AAIW (e.g. Lachkar et al., 2007, 2009). Therefore, depending on the number of eddies shed per year by the ACC, the EAC, and due to the influence of the Campbell Plateau, eddies could be making a significant contribution to the formation and properties of SAMW and to a lesser extent AAIW. A rough calculation of removing two to three CFC-12 enriched eddies from the inventory calculation, decreased the total inventory by approximate 5%, or each eddy decreased the inventory by about 2% and approximately 0.1 Sv change in the formation rate. The tracer method of CFC-12 inventories and formation rate calculations presented here takes into account all formation mechanisms contributing to SAMW and AAIW, including eddy processes.

6.3. Global comparison of mode and intermediate waters

SAMW and AAIW are an integral part of the global overturning circulation. They are formed at specific sites in the Southern Ocean and modified within each of the Atlantic, Indian, and Pacific Oceans and transported between the three oceans.

A few observational and model studies have attempted to calculate formation rates for SAMW and AAIW within the South Pacific. For a more complete comparison with other work see Table 3. Considering the substantial differences in the chosen density layers used by each study, the closest comparison can be made for SAMW with that of Qu et al. (2008). Qu et al. (2008) use high resolution CTD and ARGO profiles of differences in winter mixed layer depths to calculate an annual subduction rate for the SAMW. In the South Pacific, they estimate approximately 11.6 Sv of SAMW is formed, and this compares very well to our value of 11.7 ± 2.2 Sv. Since the calculation of Qu et al. (2008) misses much of the lower part of AAIW, the closest comparison for AAIW is with that of Sloyan and Rintoul (2001b). Sloyan and Rintoul (2001b) calculate formation rates based on inverse methods for AAIW of 4.5 Sv, compared to our value of at least 5.8 ± 1.7 Sv. Thus, these recent estimates for formation of SAMW and AAIW in the South Pacific that use physical parameters are in good agreement with the CFC-12 inventory method presented here.

SAMW and AAIW are also formed in the South Atlantic and Indian Oceans. Karstensen and Quadfasel (2002) estimate approximately 9–10 Sv of mode and intermediate waters subducted in the South Atlantic. Sloyan and Rintoul (2001b) estimate 8.4 Sv of AASW transformed into SAMW in the South Atlantic. As for the Indian Ocean, Sallee et al. (2010a) find approximately 4 Sv of light SAMW formed just in the southeast Indian Ocean. Sloyan and Rintoul (2001b) estimate 16 Sv of SAMW and 6.6 Sv of AAIW formed within the Indian Ocean. Karstensen and Quadfasel (2002) estimate approximately 22 Sv of mode water subducting in the Indian Ocean. Based on these estimates it appears that the formation of 17.5 Sv (11.7 + at least 5.8 Sv) of SAMW and AAIW within the South Pacific is greater than that formed in the Atlantic. It also appears the SAMW formation within the Indian Ocean is greater than that of the Pacific Ocean. However, the volume of the mode water layer within both the Karstensen and Quadfasel (2002) and Sloyan and Rintoul (2001b) studies is thicker and extends higher into the water column than in the Pacific. When looking at only the densest mode waters in the Indian Ocean from Karstensen and Quadfasel (2002), comparable to that of the South Pacific, the formation of SAMW in the South Pacific is greater than that of the Indian Ocean (~7 Sv).

How do the formation rates in this study of SAMW and AAIW compare with rates of formation of northern hemisphere mode and intermediate waters (Table 3)? In the North Atlantic, Labrador Sea Water (LSW) has been observed to form in as deep as 1500 m mixed

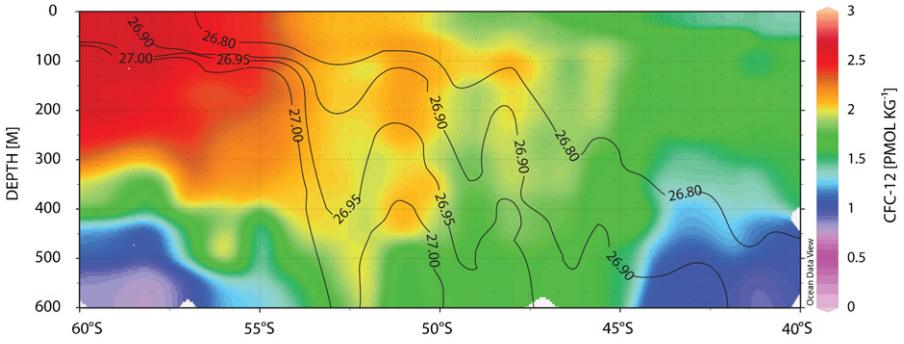

Fig. 6. Depth section along 170°W of CFC-12 concentrations in pmol kg^{-1}. Black contours represent potential density in kg m^{-3}. Cold core eddies centered around 51°S and 47°S. Note the high CFC-12 concentration within these eddies extending into SAMW density surfaces (26.8–27.06 kg m^{-3}).

Table 3
Comparison of mode and intermediate water formation rates within the literature. SAMW, Subantarctic Mode Water, AAIW, Antarctic Intermediate Water, LSW, Labrador Sea Water, CMW, Central Mode Water, NPIW, North Pacific Intermediate Water.

South Pacific water mass	Formation rate (Sv)	Author	Method	Density (kg m^{-3})
SAMW	***11.7***	***This work***	***CFC-12 inventory+geostrophic transports***	***26.80–27.06***
	9	Fine et al. (2001)	CFC ages	26.5–27.1
	11.6	Qu et al. (2008)	Annual subduction rate	26.8–27.1
	11	Marsh et al. (2000)	MICOM model	26.5–27.2
	11.4	Sloyan and Rintoul (2001b)	Inverse methods	[a]26.0–27.0 γ^n
	10.0	Macdonald et al. (2009)	Inverse methods	[a]26.2–27.1 γ^n
	7	Sallee et al. (2010a, b)	Annual subduction rate	26.8–27.0
AAIW	***5.8***	***This work***	***CFC-12 inventory***	***27.06–27.40***
	8	Fine et al. (2001)	CFC ages	27.1–27.3
	8.5	Marsh et al. (2000)	MICOM model	27.2–27.5
	4.5	Sloyan and Rintoul (2001b)	Inverse methods	[a]27.0–27.4 γ^n
	10.0	Macdonald et al. (2009)	Inverse methods	[a]27.1–27.6 γ^n
	4	Sallee et al. (2010a, b)	Annual subduction rate	27.1–27.2

Water Mass	Formation rate (Sv)	Author	Ocean Basin
LSW	7–12	Rhein et al. (2002), Kieke et al. (2006), LeBel et al. (2008)	North Atlantic
SAMW+AAIW	9–10	Karstensen and Quadfasel (2002)	South Atlantic
CMW	7.6	Ladd and Thompson (2001)	North Pacific
NPIW	2.7	Wong et al. (1998)	North Pacific
SAMW	4	Sallee et al. (2010a, b)	Indian
SAMW	16	Sloyan and Rintoul (2001b)	Indian
SAMW+AAIW	22	Karstensen and Quadfasel (2002)	Indian
AAIW	6.6	Sloyan and Rintoul (2001b)	Indian

[a] Density is in neutral density rather than sigma-theta.

layers. Using the CFC inventory method to estimate formation rates, LSW formation rates range from 7 Sv to 12 Sv and the formation is known to vary over time (Smethie and Fine, 2001; Rhein et al., 2002; Kieke et al., 2006; LeBel et al., 2008). For years with convection, LSW rates are comparable to our total SAMW formation rate of 11.7 ± 2.2 Sv and greater than the 5.8 ± 1.7 Sv lower bound estimate for AAIW formed in the southeast Pacific.

Within the North Pacific, SAMW is compared with Central Mode Water (CMW). CMW is formed via similar processes as SAMW, within winter mixed layers and is characterized by a low in potential vorticity (Oka and Suga, 2005). SAMW formation rate is greater than CMW, 11.7 ± 2.2 Sv for total SAMW and 7.6 Sv for CMW from an isopycnal model (Ladd and Thompson, 2001). North Pacific Intermediate Water (NPIW), like AAIW is a salinity minimum. Wong et al. (1998), estimate a minimum of 2.7 Sv of NPIW forming in the Okhotsk Sea. This NPIW estimate is smaller than our estimate of AAIW in the South Pacific, and this is not surprising when the CFC distributions of the two water masses are compared (Fine et al., 2001).

Total SAMW and AAIW formation rates for the South Pacific are comparable to the formation rate of LSW, and are greater than the formation rates of CMW and NPIW. SAMW and AAIW formation in the South Pacific are also greater than the formation within the Indian and Atlantic Oceans for intermediate densities. Therefore, SAMW and AAIW formed in the South Pacific make a significant contribution to the overall global formation and circulation of mode and intermediate waters. The properties of SAMW and AAIW formed in the South Pacific influence SAMW and AAIW properties within the southern hemisphere subtropical gyres. Their properties also influence global and low latitude biological export production (i.e. Marinov et al., 2006; Roemmich et al., 2007; Naveira Garabato et al., 2009).

7. Summary and conclusions

SAMW and AAIW influence the capacity of the southern hemisphere subtropical gyres to store climatologically important properties such as, heat, freshwater, and CO_2. This study presents the first wintertime observations of CFC-11 and CFC-12 saturations within SAMW (94% and 95%) and AAIW (60%, north of the SAF) within the southeast Pacific. Accurate knowledge of these winter mixed layer saturations enables the robust calculation of CFC-12 inventories within SAMW and AAIW. The CFC-12 inventory maps provide a basin-wide picture of the areas of formation of SAMW and AAIW. In the Pacific sector of the Southern Ocean the primary region of formation of SAMW and AAIW is the southeast Pacific. The inventory maps provide direct evidence that SAMW also has another major area of formation in the central Pacific, as proposed by McCartney (1982). Higher CFC-12 inventories in eddies in the central Pacific are suggestive of higher local formation rates for SAMW, and to a lesser extent for AAIW. The CFC-12 inventories are used to calculate formation rates for SAMW at 7.3 ± 2.1 Sv and 5.8 ± 1.7 Sv for AAIW that circulate within the South Pacific subtropical gyre. Based on a transport of 4.4 Sv from the South Pacific through the Drake Passage, the total formation rate of SAMW in the South Pacific is 11.7 ± 2.2 Sv. The AAIW formation rate of 5.8 ± 1.7 Sv is a lower bound on the formation of AAIW within the South Pacific, as we cannot estimate the volume transport of newly formed AAIW through the Drake Passage. The CFC-derived formation rates represent the average water mass formation rates over the period from 1970 to 2005, and take into account all formation processes, including eddies, winter convection, and mixing. SAMW and AAIW formation in the South Pacific represent a major portion of the mode and intermediate water formation worldwide. This study provides a multi-decadal average of SAMW and AAIW formation rates, providing a baseline with which to compare past and future formation rates of SAMW and AAIW.

Acknowledgments

C.A. Hartin and R.A. Fine thank the National Science Foundation OCE O7-52980, 04-24744 and OCE 02-23951 for support. L. D. Talley and T. K. Chereskin thank the National Science Foundation OCE-032754 for support. B. M. Sloyan's

contribution to this work was undertaken as part of the Australian Climate Change Science Program, funded jointly by the Department of Climate Change and Energy Efficiency and CSIRO. We thank Donald Olson for contributing to our understanding of the role of eddies in formation of Mode Waters.

References

Broecker, W.S., Peng, T.H., Mathieu, G., Hesslein, R., Torgersen, T., 1980. Gas exchange rate measurements in a natural system. Radiocarbon 22, 676–683.

Chereskin, T., 2005. Preliminary Cruise Report. CLIVAR; Carbon Hydrographic Data Office. 〈http://cchdo.uscd.edu〉 (accessed 〈http://www.pord.ucsd.edu/~ltalley/aaiw/nodc_submit/aaiw_2005_combined_cruisereport.pdf〉).

Cunningham, S.A., Alderson, S.G., King, B.A., Brandon, M.A., 2003. Transport and variability of the Antarctic circumpolar current in Drake Passage. Journal of Geophysical Research 108 (C5), 8084.

Dickson, R., Lazier, J., Meincke, J., Rhines, P., Swift, J., 1996. Long-term coordinated changes in the convective activity of the North Atlantic. Progress in Oceanography 38 (3), 241–295.

Doney, S.C., Bullister, J.L., 1992. A chlorofluorocarbon section in the eastern North Atlantic. Deep Sea Research Part I. Oceanographic Research Papers 39 (11–12), 1857–1883.

Fine, R.A., 2011. Observations of CFCs and SF6 as ocean tracers. Annual Review of Marine Science 3 (1), 173–195.

Fine, R.A., Maillet, K.A., Sullivan, K.F., Willey, D., 2001. Circulation and ventilation flux of the Pacific Ocean. J. Geophys. Res. 106 (C10), 22159–22178.

Fine, R.A., Rhein, M., Andrié, C., 2002. Using a CFC effective age to estimate propagation and storage of climate anomalies in the deep western North Atlantic Ocean. Geophysics Research Letters 29 (24), 2227–2230.

Fine, R.A., Warner, M.J., Weiss, R.F., 1988. Water mass modification at the Agulhas retroflection: chlorofluoromethane studies. Deep Sea Research Part I. Oceanographic Research Papers 35 (3), 311–332.

Firing, Y.L., Chereskin, T.K., Mazloff, M.R., Vertical structure and transport of the antarctic circumpolar current in drake passage from direct velocity observations. Journal of Geophysical Research, submitted for publication.

Francois, R., Altabet, M.A., Yu, E.-F., Sigman, D.M., Bacon, M.P., Frank, M., Bohrmann, G., Bareille, G., Labeyrie, L.D., 1997. Contribution of Southern Ocean surface-water stratification to low atmospheric CO2 concentrations. Nature 389 (6654), 929–935.

Gille, S.T., Yale, M.M., Sandwell, D.T., 2000. Global correlation of mesoscale ocean variability with seafloor roughness from satellite altimetry. Geophys. Res. Lett. 27 (9), 1251–1254.

Hall, A., Visbeck, M., 2002. Synchronous variability in the Southern Hemisphere atmosphere, sea ice, and ocean resulting from the Annular Mode. Journal of Climate 15 (21), 3043–3057.

Hanawa, K., Talley, L.D., 2001. Mode Waters. In: Siedler, G., Church, J., Gould, J. (Eds.), Ocean Circulation and Climate. Academic Press, pp. 373–386.

Herraiz-Borreguero, L., Rintoul, S.R., 2010. Subantarctic Mode Water variability influenced by mesoscale eddies south of Tasmania. Journal of Geophysical Research 115 (C4), C04004 1–12.

Holte, J., Talley, L.D., Chereskin, T.K., Sloyan, B.M., The role of air-sea fluxes in Subantarctic Mode Water formation. Journal of Geophysical Research, submitted for publication.

Iudicone, D., Rodgers, K.B., Schopp, R., Madec, G., 2007. An exchange window for the injection of Antarctic intermediate water into the South Pacific. Journal of Physical Oceanography 37 (1), 31–49.

Karstensen, J., Quadfasel, D., 2002. Formation of Southern Hemisphere thermocline waters: water mass conversion and subduction. Journal of Physical Oceanography 32 (11), 3020–3038.

Karstensen, J., Quadfasel, D., 2002. Water subducted into the Indian Ocean subtropical gyre. Deep Sea Research Part II: Topical Studies in Oceanography 49 (7–8), 1441–1457.

Kieke, D., Rhein, M., Stramma, L., Smethie, W.M., LeBel, D.A., Zenk, W., 2006. Changes in the CFC inventories and formation rates of Upper Labrador Sea Water, 1997–2001. Journal of Physical Oceanography 36, 64–86.

Koshlyakov, M.N., Tarakanov, R.Y., 2005. Intermediate water masses in the southern part of the Pacific Ocean. Oceanology 45 (4), 455–473.

Lachkar, Z., Orr, J.C., Dutay, J.-C., Delecluse, P., 2007. Effects of mesoscale eddies on global ocean distributions of CFC-11, CO2, and delta 14C. Ocean Science 3, 461–482.

Lachkar, Z., Orr, J.C., Dutay, J.-C., Delecluse, P., 2009. On the role of mesoscale eddies in the ventilation of Antarctic intermediate water. Deep Sea Research Part I: Oceanographic Research Papers 56 (6), 909–925.

Ladd, C., Thompson, L., 2001. Water mass formation in an isopycnal model of the North Pacific. Journal of Physical Oceanography 31 (6), 1517–1537.

Lazier, J., Hendry, R., Clarke, A., Yashayaev, I., Rhines, P., 2002. Convection and restratification in the Labrador Sea, 1990–2000. Deep Sea Research Part I: Oceanographic Research Papers 49 (10), 1819–1835.

LeBel, D.A., Smethie Jr, W.M., Rhein, M., Kieke, D., Fine, R.A., Bullister, J.L., Min, D.-H., Roether, W., Weiss, R.F., Andrié, C., Smythe-Wright, D., Peter Jones, E., 2008. The formation rate of North Atlantic Deep Water and eighteen degree water calculated from CFC-11 inventories observed during WOCE. Deep Sea Research Part I: Oceanographic Research Papers 55 (8), 891–910.

Macdonald, A.M., Mecking, S., Robbins, P.E., Toole, J.M., Johnson, G.C., Talley, L., Cook, M., Wijffels, S.E., 2009. The WOCE-era 3-D Pacific Ocean circulation and heat budget. Progress in Oceanography 82, 281–325.

Marinov, I., Gnanadesikan, A., Toggweiler, J.R., Sarmiento, J.L., 2006. The Southern Ocean biogeochemical divide. Nature 441, 964–967.

Marsh, R., Nurser, A.J.G., Megann, A.P., New, A.L., 2000. Water mass transformation in the Southern Ocean of a global isopycnal coordinate GCM. Journal of Physical Oceanography 30 (5), 1013–1045.

Marshall, G.J., 2003. Trends in the Southern annular mode from observations and reanalyses. Journal of Climate 16 (24), 4134–4143.

McCartney, M.S., 1977. A Voyage of Discovery, George Deacon 70th Anniversary Volume. In: Angel, M. (Ed.), Subantarctic Mode Water. Pergamon Press, pp. 103–119.

McCartney, M.S., 1982. The subtropical recirculation of mode waters. Journal of Marine Research 40 (Supplement), 427–464.

Morrow, R., Donguy, J.-R., Chaigneau, A., Rintoul, S.R., 2004. Cold-core anomalies at the subantarctic front, south of Tasmania. Deep Sea Research Part I: Oceanographic Research Papers 51 (11), 1417–1440.

Naveira Garabato, A.C., Jullion, L.c., Stevens, D.P., Heywood, K.J., King, B.A., 2009. Variability of Subantarctic mode water and Antarctic Intermediate Water in the Drake Passage during the late-twentieth and early-twenty-first centuries. Journal of Climate 22 (13), 3661–3688.

Naveira Garabato, A.C., Stevens, D.P., Heywood, K.J., 2003. Water mass conversion, fluxes, and mixing in the Scotia Sea diagnosed by an inverse model. Journal of Physical Oceanography 33 (12), 2565–2587.

Oka, E., Suga, T., 2005. Differential formation and circulation of North Pacific Central mode water. Journal of Physical Oceanography 35 (11), 1997–2011.

Olson, D.B., Emery, J.W., 1978. Eddies and ridges in the thermal structure south of New Zealand. Antarctic Journal, 79–91.

Olson, D.B., Fine, R., Gordon, A.L., 1992. Convective modification of water masses in the Agulhas. Deep Sea Research I 39, S163–S181.

Orsi, A.H., Whitworth, T., Nowlin Jr., W.P., 1995. On the meridional extent and fronts of the Antarctic circumpolar current. Deep-Sea Research 42, 641–673.

Orsi, A.H., Johnson, G.C., Bullister, J.L., 1999. Circulation, mixing, and production of Antarctic bottom water. Progress in Oceanography 43 (1), 55–109.

Phillips, H.E., Rintoul, S.R., 2000. Eddy variability and energetics from direct current measurements in the Antarctic Circumpolar current South of Australia. Journal of Physical Oceanography 30 (12), 3050–3076.

Qiu, B., Huang, R.X., 1995. Ventilation of the North Atlantic and North Pacific: subduction versus obduction. Journal of Physical Oceanography, 25.

Qu, T., Gao, S., Fukumori, I., Fine, R.A., Lindstrom, E.J., 2008. Subduction of South Pacific waters. Geophysical Research Letters 35 (2), L02610 1–6.

Reid, J.L., 1965. Intermediate Waters of the Pacific Ocean. The Johns Hopkins Oceanographic Studies 2, 85.

Rhein, M., Fischer, J., Smethie, W.M., Smythe-Wright, D., Weiss, R.F., Mertens, C., Min, D.H., Fleischmann, U., Putzka, A., 2002. Labrador Sea Water: pathways, CFC inventory, and formation rates. Journal of Physical Oceanography 32 (2), 648–665.

Ridgway, K.R., Dunn, J.R., 2007. Observational evidence for a Southern Hemisphere oceanic supergyre. Geophysical Research Letters 34 (L13612), 1–5.

Roemmich, D., Gilson, J., Davis, R., Sutton, P., Wijffels, S., Riser, S., 2007. Decadal spinup of the South Pacific subtropical gyre. Journal of Physical Oceanography 37 (2), 162–173.

Sabine, C.L., Feely, R.A., Gruber, N., Key, R.M., Lee, K., Bullister, J.L., Wanninkhof, R., Wong, C.S., Wallace, D.W.R., Tilbrook, B., Millero, F.J., Peng, T.-H., Kozyr, A., Ono, T., Rios, A.F., 2004. The Oceanic sink for Anthropogenic CO_2. Science 305 (5682), 367–371.

Sallee, J.B., Speer, K., Rintoul, S., Wijffels, S., 2010a. Southern Ocean thermocline ventilation. Journal of Physical Oceanography 40 (3), 509–529.

Sallee, J.B., Speer, K.G., Rintoul, S.R., 2010b. Zonally asymmetric response of the Southern Ocean mixed-layer depth to the Southern Annular Mode. Nature Geosci 3 (4), 273–279.

Schmitz, W.J., 1996. On the world ocean circulation, vol. II: The Pacific and Indian Oceans. A Global update.

Siegenthaler, U., Wenk, T., 1984. Rapid atmospheric CO_2 variations and ocean circulation. Nature 308 (5960), 624–626.

Sloyan, B.M., Rintoul, S.R., 2001a. The Southern Ocean limb of the global deep overturning circulation. Journal of Physical Oceanography 31, 143–173.

Sloyan, B.M., Rintoul, S.R., 2001b. Circulation, renewal, and modification of Antarctic Mode and Intermediate Water. Journal of Physical Oceanography 31, 1005–1030.

Sloyan, B.M., Talley, L.D., Chereskin, T.K., Fine, R., Holte, J., 2010. Antarctic Intermediate Water and Subantarctic Mode Water formation in the southeast Pacific: the role of turbulent mixing. Journal of Physical Oceanography 40 (7), 1558–1574.

Smethie, W.M., Fine, R.A., 2001. Rates of North Atlantic Deep Water formation calculated from chlorofluorocarbon inventories. Deep Sea Research Part I: Oceanographic Research Papers 48 (1), 189–215.

Smethie, W.M., Fine, R.A., Putzka, A., Jones, E.P., 2000. Tracing the flow of North Atlantic Deep Water using chlorofluorocarbons. Journal of Geophysical Research 105 (C6), 14,297–14,323.

Talley, L.D., 1996. Antarctic intermediate water in the South Atlantic. In: Wefer, G., Berger, H.H., Siedler, G., Webb, D. (Eds.), The South Atlantic: Present and Past Circulation. Springer-Verlag.

Talley, L.D., 2003. Shallow, intermediate, and deep overturning components of the global heat budget. Journal of Physical Oceanography 33 (3), 530–560.
Talley, L.D., 2008. Freshwater transport estimates and the global overturning circulation: Shallow, deep and throughflow components. Progress in Oceanography 78 (4), 257–303.
Toggweiler, J.R., 1999. Variation of atmospheric CO_2 by ventilation of the ocean's deepest water. Paleoceanography 14 (5), 571–588.
Tsuchiya, M., Talley, L.D., 1998. A Pacific hydrographic section at 88 W: water-property distribution. Journal of Geophysical Research 103, 12,899–12,918.
Walker, S.J., Weiss, R.F., Salameh, P.K., 2000. Reconstructed histories of the annual mean atmospheric mole fractions for the halocarbons CFC-11, CFC-12, CFC-113, and carbon tetrachloride. Journal of Geophysical Research 105 (C6), 14285–14296.
Wallace, D.W.R., Lazier, J.R.N., 1988. Anthropogenic chlorofluoromethanes in newly formed Labrador Sea water. Nature 332 (6159), 61–63.
Warner, M.J., Weiss, R.F., 1985. Solubilities of chlorofluorocarbons 11 and 12 in water and seawater. Deep-Sea Research 32 (12), 1485–1497.
Waugh, D.W., Abraham, E.R., 2008. Stirring in the global surface ocean. Geophys. Res. Lett. 35 (20), L20605 1–5.
Willey, D.A., Fine, R.A., Sonnerup, R.E., Bullister, J.L., Smethie Jr., W.M., Warner, M.J., 2004. Global oceanic chlorofluorocarbon inventory. Geophys. Res. Lett. 31 (1), L01303 1–4.
Wolberg, J.R., 1967. Prediction Analysis, Inc. D. Van Nostrand Company.
Wong, C.S., Matear, R.J., Freeland, H.J., Whitney, F.A., Bychkov, A.S., 1998. WOCE line P1W in the Sea of Okhotsk 2. CFCs and the formation rate of intermediate water. Journal of Geophysical Research 103, 15625–15642.